

Full Paper

Strategy for Low Background-Current Levels in the Electrochemical Biosensors Using Horse-Radish Peroxidase Labels

Hyun Ju Kang, Md. Abdul Aziz, Boyoun Jeon, Kyungmin Jo, Haesik Yang*

Department of Chemistry and Chemistry Institute for Functional Materials, Pusan National University, Busan 609-735, Korea

*e-mail: hyang@pusan.ac.kr

Received: May 17, 2009

Accepted: August 8, 2009

Abstract

This article describes an electrochemical strategy to achieve low background-current levels in horse-radish peroxidase (HRP)-based electrochemical immunosensors. The strategy consists of (i) the use of an HRP substrate/product redox couple whose formal potential is high and (ii) the use of an electrode that shows moderate electrocatalytic activity for the redox couple. The strategy is proved by a model biosensor using a catechol/*o*-benzoquinone redox couple and an indium tin oxide (ITO) electrode. The combined effect of high formal potential and moderate electrocatalytic activity allows *o*-benzoquinone electroreduction with minimal catechol electrooxidation and H₂O₂ electroreduction. The detection limit for mouse-IgG is 100 pg/mL.

Keywords: Catechol, Indium tin oxide, Horse-radish peroxidase, Immunosensors, Biosensors, Enzymes

DOI: 10.1002/elan.200900257

1. Introduction

In enzyme-based electrochemical biosensors, horse-radish peroxidase (HRP) [1–6] and alkaline phosphatase (ALP) [7–14] are commonly used as signal-amplifying catalytic labels. Generally, reaction products of the enzyme are electroreduced in HRP-based biosensors, but electrooxidized in ALP-based biosensors to generate electrochemical signals. In electrochemical detection, HRP-based sensors have the distinct disadvantage over ALP-based sensors, in that the background-current levels in HRP-based sensors are higher and less reproducible than in ALP-based sensors, making it difficult to achieve low detection limits. Most substrates of HRP (e.g., hydroquinone (HQ)) are highly electroactive within an electrochemical potential window [1–6], whereas substrates of ALP (e.g., 1-naphthyl phosphate) are much less electroactive [7, 15]. Accordingly, electroactive interfering substrates can significantly affect background-current levels in HRP-based sensors. Moreover, the hydrogen peroxide (H₂O₂) necessarily used as an oxidizing agent in HRP catalysis is easily electroreduced within an electrochemical potential window and, as a result, H₂O₂ electroreduction substantially increases background-current levels. Electroreduction of dissolved oxygen (O₂) can also increase the background-current level, if highly electrocatalytic electrodes are used as the working electrodes. Therefore, it is crucial to minimize the background-current level caused by redox reactions of the substrate, H₂O₂, and O₂, to achieve high sensitivities in HRP-based electrochemical sensors.

Phenolic compounds such as HQ [1, 2] and catechol (CT) [16–18] have been widely used as substrates for HRP,

because their enzymatic reactions are very fast and their products are readily measured. On highly electrocatalytic electrodes, electron-transfer kinetics for both the substrate and product is also very fast, such that, in potential-sweep methods, such as cyclic voltammetry, it is difficult to electroreduce a product near its formal potential without electrooxidation of the substrate. On the other hand, moderately electrocatalytic electrodes, slower electron-transfer kinetics induces higher overpotentials for both substrate electrooxidation and product electroreduction, which, in turn, allows the separation of two potential regions of substrate electrooxidation and product electroreduction in potential-sweep measurements. Thus, electroreduction of the product is feasible without electrooxidation of the substrate on moderately electrocatalytic electrodes. Furthermore, moderately electrocatalytic electrodes allow high overpotentials for H₂O₂ and O₂ electroreduction, which could lower the influence of H₂O₂ and O₂ on background-current levels.

Indium tin oxide (ITO) electrodes exhibit moderately electrocatalytic activities for phenolic compounds [19], show a low, flat, capacitive current behavior over a wide range of potentials [20–22], and show high overpotentials for H₂O₂ and O₂ electroreduction, characteristics which are suitable for the selective electrochemical measurement of a product in the presence of a substrate, H₂O₂, and O₂. Along with a moderately electrocatalytic electrode, it is desirable to use a substrate/product redox couple whose formal potential is higher, in which case the electroreduction of product occurs at potentials more positive than the H₂O₂ and O₂ electroreduction. It is known that the formal potential of a CT/*o*-benzoquinone redox couple is higher

than that of a HQ/*p*-benzoquinone couple [23, 24]. For example, in phosphate buffered saline (PBS) (pH 6.8), the formal potential of a CT/*o*-benzoquinone redox couple is ca. 0.39 V vs. SCE, while the formal potential of a HQ/*p*-benzoquinone couple is ca. 0.29 V [23]. In particular, CT as a substrate may serve better for lower background-current levels than HQ, the most common substrate in HRP-based sensors.

In this study, a novel strategy is presented to achieve low background-current levels in electrochemical immunosensors based on HRP. First, cyclic voltammograms of CT and HQ on dendrimer-modified ITO electrodes were investigated in terms of selective electrochemical measurements of a product in the presence of a substrate and cyclic voltammograms of H₂O₂ were examined in terms of low background-current levels. Second, the dependence of cyclic voltammograms on the concentration of target mouse-IgG was examined when CT or HQ was used as a substrate. And finally, the detection limit of each case was determined and compared.

2. Experimental

2.1. Materials and Reagents

ITO-coated glasses were supplied by Geomatec (Japan); absolute ethanol purchased from Fisher Scientific; and trichloroethylene, H₂O₂, NH₄OH, methanol, CT, HQ, 3-phosphonopropionic acid (PPA), *N*-(3-dimethylamino-propyl)-*N*-ethylcarbodiimide hydrochloride (EDC), *N*-hydroxysuccinimide (NHS), *N,N*-dimethylformamide and amine terminated G4 poly(amidoamine) dendrimer received from Aldrich. (+)-Biotin-NHS, streptavidin, biotinylated goat antimouse-IgG, mouse-IgG from serum, and HRP-conjugated goat antimouse-IgG were supplied by Sigma-Aldrich. All buffer reagents were obtained from Sigma, Aldrich, or Fluka, used as received, and all aqueous solutions prepared in doubly distilled water.

The PBS solution consisted of 0.01 M phosphate, 0.138 M NaCl, and 0.0027 M KCl (pH 7.4). The PBSB buffer solution was PBS with 1% (w/v) albumin-bovine serum added. The rinsing buffer (RB) solution consisted of 50 mM tromethamine, 40 mM HCl, 0.5 M NaCl, and 0.05% (w/v) albumin-bovine serum (pH 7.6).

2.2. Construction of Immunosensing Layers

ITO electrodes were successively cleaned with trichloroethylene, ethanol, and water, dried at 50 °C, and pretreated in a mixture of 5:1:1 H₂O/H₂O₂ (30%)/NH₄OH (30%) (v/v/v) at 70 °C for 1.5 h. After washing with copious amounts of water and drying at 50 °C, the electrodes were immersed in an aqueous solution of 0.1 mM PPA for 36 h to form a carboxylic-acid-functionalized monolayer. The carboxylic groups were activated with an aqueous solution of 50 mM EDC and 25 mM NHS for 2 h. Methanol with 100 μM

amine-terminated G4 poly(amidoamine) dendrimer was dropped onto the electrodes, and then the electrodes were kept in undisturbed conditions for 2 h. After removing the nonspecifically adsorbed dendrimers with a PBS rinse, the electrodes were immersed in a *N,N*-dimethylformamide solution containing 1.5 mg/mL (+)-biotin-NHS for 2 h to immobilize the biotin, washed with methanol and water, immersed in PBS containing 100 μg/mL streptavidin for 30 min, and washed twice with PBS. The electrodes were then dipped in a PBSB solution containing 0.05% (v/v) Tween-20 (pH 7.4) for 30 min to remove nonspecifically bound proteins, washed with RB, incubated for 30 min in PBSB containing 100 μg/mL biotinylated goat antimouse-IgG, and washed with RB. The electrodes were then treated in a PBSB solution containing different concentrations of mouse-IgG, washed with RB, incubated for 30 min in a PBSB solution containing 10 μg/mL HRP-conjugated goat antimouse-IgG, and washed with RB.

2.3. Electrochemical and Immunosensing Experiments

The electrochemical experiments were performed using a CHI 405A instrument (CH instruments, USA) and an electrochemical cell consisting of a modified ITO working electrode, a Pt counter electrode, and an Ag/AgCl (3 M NaCl) reference electrode. The geometric area of the working electrode was 0.28 cm². For the immunosensing experiments, the cell was filled with a PBS solution containing 1.0 mM H₂O₂ and 1.0 mM CT or HQ and kept in undisturbed condition during enzymatic reaction (10 min). All voltammograms were obtained without removal of dissolved O₂ from solutions. The experiment at each mouse-IgG concentration was repeated five times by using different immunosensing working electrodes.

3. Results and Discussion

3.1. Electrochemical Strategy for Low Background-Current Levels

Figure 1 shows schematic cyclic voltammograms for a substrate/product redox couple and H₂O₂ on highly electrocatalytic electrodes (Fig. 1a) and schematic cyclic voltammograms on the electrodes suitable for low background-current levels (Fig. 1b). In HRP-based sensors, HRP converts a reduced substrate (Red) to an oxidized product (Ox). The converted Ox should be selectively electroreduced to obtain high signal-to-background ratios. If an electrode is highly electrocatalytic for the electrochemical reaction of Red and Ox, the potential difference between anodic and cathodic peaks is small in a cyclic voltammogram for the Red/Ox redox couple and the electroreduction of H₂O₂ occurs at low overpotentials (Fig. 1a). When potential (i) is applied, Red electrooxidation along with Ox electroreduction occurs and, when potential (ii) is applied, H₂O₂ electroreduction as well as Ox electroreduction takes place.

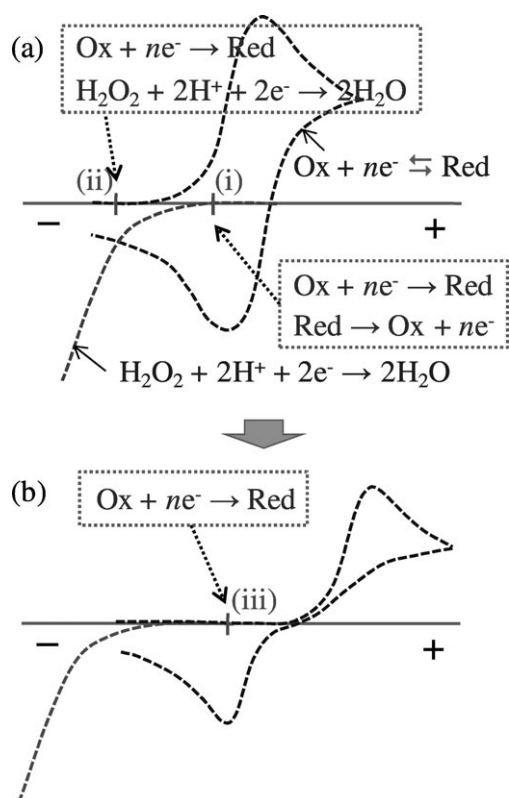


Fig. 1. (a) Schematic cyclic voltammograms for a substrate/product redox couple and H_2O_2 on highly electrocatalytic electrodes and (b) schematic cyclic voltammograms on the electrodes suitable for low background-current levels. Blue and red curves are voltammograms for the redox couple and H_2O_2 , respectively. Red represents a reduced substrate, and Ox represents an oxidized product.

In both cases, selective Ox electroreduction is not possible. If an electrode is moderately electrocatalytic, the potential difference between anodic and cathodic peaks is large (Fig. 1b) and the electroreduction of H_2O_2 occurs at higher overpotentials (Fig. 1b). Moderate electrocatalytic activity of an electrode induces high overpotentials for both Red electrooxidation and Ox electroreduction. When potential iii is applied, only Ox electroreduction occurs, and there is no Red electrooxidation and H_2O_2 electroreduction at this potential. If the formal potential of a Red/Ox redox couple is higher, selective Ox electroreduction is feasible over a wider range of potentials.

3.2. Electrocatalytic Properties of Dendrimer-modified ITO Electrodes

The electrocatalytic property of dendrimer-modified ITO electrodes for a CT/*o*-benzoquinone redox couple and a HQ/*p*-benzoquinone redox couple were examined by cyclic voltammograms obtained on dendrimer-modified ITO electrodes in a PBS solution containing CT or HQ (Fig. 2a). In our previous studies, the electrocatalytic properties of ITO electrodes were improved by partial

modification of ITO electrodes with ferrocene [11], carbon nanotubes [12], or gold nanoparticles [13]. In this study, the intrinsic low electrocatalytic activity of ITO electrodes was utilized by not modifying ITO electrodes with electrocatalytic materials.

In a cyclic voltammogram for a CT/*o*-benzoquinone couple, anodic and cathodic peaks appeared at 0.49 and -0.08 V, respectively (Fig. 2a), the large difference between the two peak potentials indicating moderately low electrocatalytic activity of the ITO electrodes. Only CT electrooxidation occurred at potentials more positive than ~ 0.2 V, whereas only *o*-benzoquinone electroreduction occurred at potentials more negative than ~ 0.1 V. In contrast, in a cyclic voltammogram for a HQ/*p*-benzoquinone couple, an anodic and cathodic peaks appeared at 0.8 and -0.35 V, respectively (Fig. 2a), both more positive and more negative, respectively, than for the CT/*o*-benzoquinone couple. Although selective *p*-benzoquinone electroreduction was readily achieved at potentials more negative than 0.0 V, *p*-benzoquinone electroreduction occurred at potentials more negative than *o*-benzoquinone electroreduction. This

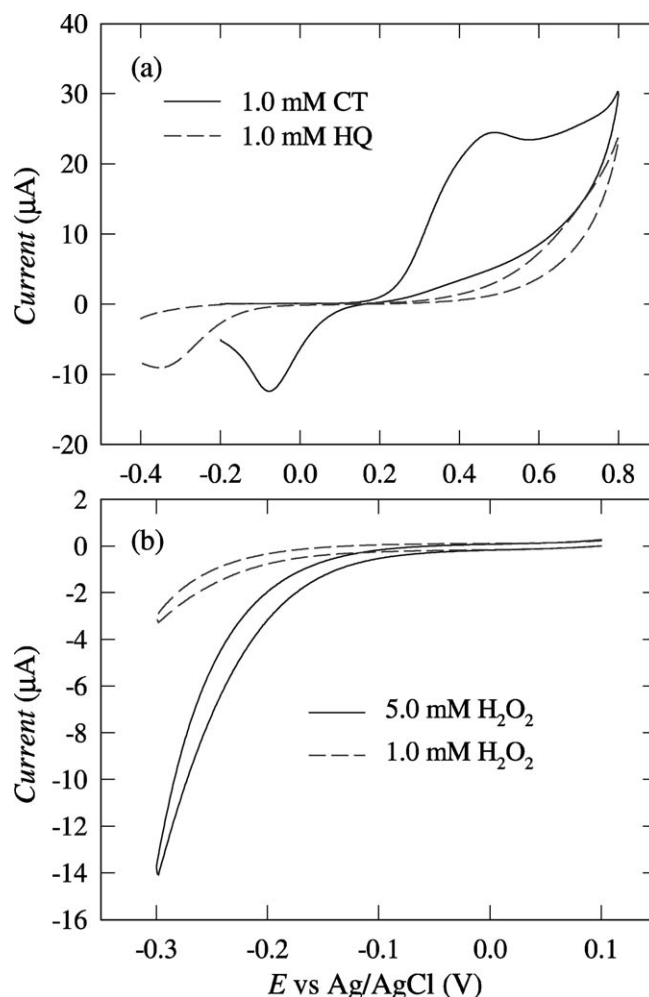


Fig. 2. Cyclic voltammograms obtained in (a) a PBS solution containing 1.0 mM CT or 1.0 mM HQ and (b) a PBS solution containing 1.0 mM or 5.0 mM H_2O_2 on dendrimer-modified ITO electrodes.

result was attributed to the very low electrocatalytic activity of ITO electrodes for the HQ/*p*-benzoquinone couple [19], and partially to the lower formal potential of a HQ/*p*-benzoquinone couple relative to a CT/*o*-benzoquinone couple [23, 24].

The electrocatalytic property of ITO electrodes for H₂O₂ electroreduction was examined by cyclic voltammograms recorded in a PBS solution containing 1.0 mM or 5.0 mM H₂O₂ on dendrimer-modified ITO electrodes (Fig. 2b). H₂O₂ electroreduction was low at potentials more positive than -0.1 V in a 1.0 mM H₂O₂-containing solution (Fig. 2b). *o*-Benzoquinone electroreduction was substantial at potentials more positive than -0.1 V (Fig. 2a), but *p*-benzoquinone electroreduction was negligible (Fig. 2a). Thus, *o*-benzoquinone electroreduction along with minimal H₂O₂ electroreduction was possible at potentials more positive than -0.1 V, but *p*-benzoquinone electroreduction with minimal H₂O₂ electroreduction was not possible. These results showed that the moderately low electrocatalytic activity of ITO electrodes for a CT/*o*-benzoquinone couple and higher formal potentials of the couple enabled selective *o*-benzoquinone electroreduction with minimal CT and H₂O₂ electrooxidation.

When a 5.0 mM H₂O₂ solution was used, the cathodic current of H₂O₂ was higher than in a 1.0 mM solution. If a low concentration of H₂O₂ is used in HRP-based electrochemical sensors, the background-current level caused by H₂O₂ electroreduction is low, whereas the enzymatic reaction by HRP is slow. In this study, 1.0 mM H₂O₂ was selected to obtain both high enzymatic reaction rates and low background-current levels.

3.3. Electrochemical Immunosensors for Mouse-IgG

Figure 3 shows a schematic diagram of a HRP-based electrochemical biosensor that detects mouse-IgG. Antimouse-IgG-modified ITO electrodes were obtained by immobilizing biotinylated antimouse-IgG on streptavidin- and dendrimer-modified ITO electrodes. The dendrimer layer allowed low levels of nonspecific binding of proteins and, importantly, highly reproducible, functionalized surfa-

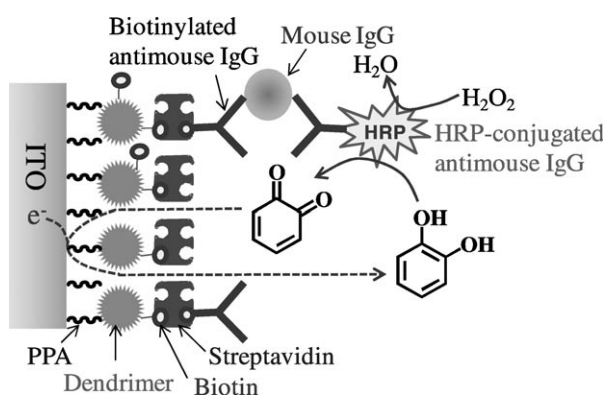


Fig. 3. Schematic diagram for a HRP-based electrochemical biosensor that detects mouse-IgG.

ces. Target mouse-IgG was captured by antimouse-IgG on the modified ITO electrodes, and HRP-conjugated antimouse-IgG was bound to the captured mouse-IgG. The HRP then converted CT (or HQ) into *o*-benzoquinone (or *p*-benzoquinone) in the presence of H₂O₂, and the enzymatically amplified *o*-benzoquinone (or *p*-benzoquinone) was electroreduced to obtain electrochemical signals.

Linear sweep voltammograms, obtained at zero and various concentrations of mouse-IgG in an immunosensor using CT substrate (Fig. 4a), showed that CT electrooxidation was negligible at potentials more negative than 0.1 V (Fig. 2a) and, thus, 0.1 V was chosen as the starting potential in linear sweep voltammograms. The cathodic current of *o*-benzoquinone increased with increasing concentrations of

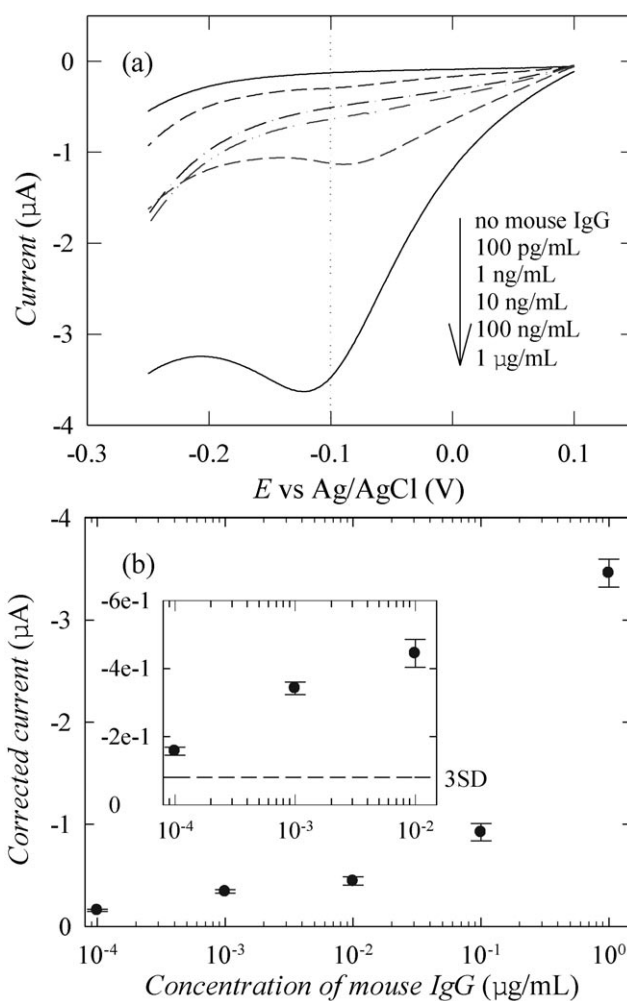


Fig. 4. (a) Dependence of linear sweep voltammograms on the concentration of mouse-IgG when CT is used as a substrate. Voltammograms were obtained at a scan rate of 20 mV/s after incubation for 10 min in a PBS solution (pH 7.4) containing 1.0 mM CT and 1.0 mM H₂O₂ at 0, 100 pg/mL, 1, 10, 100 ng/mL, and 1 µg/mL mouse-IgG. (b) Calibration curve for cathodic currents at -0.1 V in (a). All data were subtracted by the mean current at a concentration of zero mouse-IgG. The inset represents a magnification of the data points obtained at low IgG concentrations. The dashed line corresponds to three times the standard deviation (SD) at zero concentration.

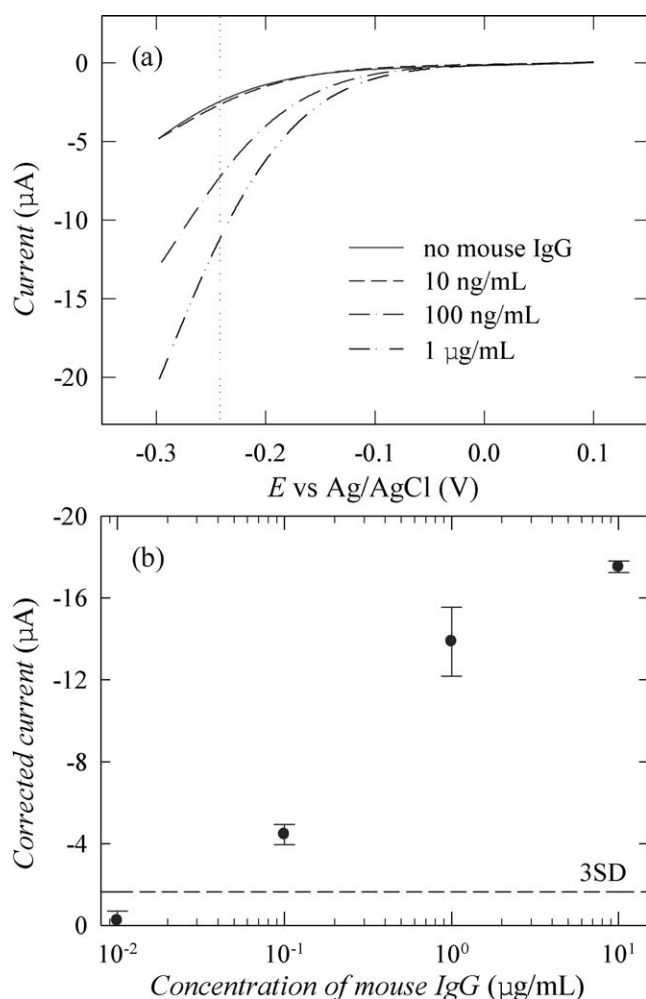


Fig. 5. (a) Dependence of linear sweep voltammograms on the concentration of mouse-IgG when HQ is used as a substrate. Voltammograms were obtained at a scan rate of 20 mV/s after incubation for 10 min in a PBS solution (pH 7.4) containing 1.0 mM HQ and 1.0 mM H_2O_2 at 0, 10, 100 ng/mL, and 1 $\mu\text{g/mL}$ mouse-IgG. (b) Calibration curve for cathodic currents at -0.24 V in (a). All data were subtracted by the mean current at a concentration of zero mouse-IgG. The dashed line corresponds to three times the standard deviation (SD) at zero concentration.

mouse-IgG and, at zero concentration of mouse-IgG, the current behavior was almost similar to that of antimouse-IgG-modified ITO electrodes (figure not shown). This result indicated that nonspecific binding of HRP-conjugated antimouse-IgG was very low.

Linear sweep voltammograms in an immunosensor using HQ substrate were also obtained (Fig. 5a). Considering that HQ electrooxidation was negligible at potentials more negative than 0.2 V (Fig. 2a), 0.1 V was chosen as the starting potential. Because p -benzoquinone electroreduction required high overpotentials, p -benzoquinone electroreduction occurred in a potential region where H_2O_2 electroreduction was considerable. In this case, it is not easy to achieve high signal-to-background ratios.

The calibration plot for the immunosensor using CT substrate is shown in Figure 4b. The dependence of cathodic currents at -0.1 V in Fig. 4a on the concentration of mouse-IgG is plotted in Figure 4b. Because the peak potentials of CT electroreduction occurred near -0.1 V (Fig. 2a and Fig. 4a) and the cathodic current of H_2O_2 was low at this potential (Fig. 2b), a potential of -0.1 V was chosen to obtain high signal-to-background ratios in the calibration plot. The current at 0.1 ng/mL mouse-IgG was higher than at zero mouse-IgG (Fig. 4b) and, thus, the detection limit for mouse-IgG in the immunosensor using CT substrate was ca. 0.1 ng/mL.

The calibration plot for the immunosensor using HQ substrate is also shown in Figure 5b. The cathodic current of HQ was negligible at -0.1 V, the cathodic peak of HQ appeared at ca. -0.35 V (Fig. 2a), and the cathodic current of H_2O_2 was considerable at -0.35 V (Fig. 2b). Considering them, a potential of -0.24 V was chosen to obtain high signal-to-background ratios in the calibration plot. The current at 100 ng/mL mouse-IgG was higher than that at zero mouse-IgG, but the current at 10 ng/mL mouse-IgG was similar to that at zero mouse-IgG (Fig. 5b). The calculated detection limit for mouse-IgG was ca. 100 ng/mL, which was ca. 1,000-times higher than the detection limit in the immunosensor using CT substrate (0.1 ng/mL). The higher redox potential of a CT/ o -benzoquinone couple and the moderate electrocatalytic activity of ITO electrodes for this couple enabled us to achieve a low background-current level, resulting in a low detection limit. This result clearly shows that low background-current levels are crucial in achieving low detection limits.

4. Conclusions

An electrochemical strategy was presented for producing low background-current levels in HRP-based electrochemical immunosensors. The use of (i) a redox couple whose formal potential is high (CT/ o -benzoquinone) and (ii) an electrode that shows moderate electrocatalytic activity for the redox couple (ITO electrode) enabled o -benzoquinone electroreduction with minimal CT electrooxidation and H_2O_2 electroreduction and produced high signal-to-background ratios. The appropriate design of a substrate through consideration of this electrochemical strategy could allow the development of biosensors with much lower detection limits.

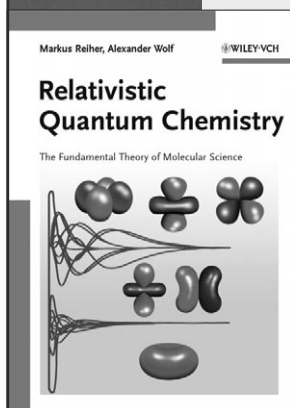
5. Acknowledgements

This work was supported by The Nano/Bio Science & Technology Program (2005-01333) of the Ministry of Education, Science, and Technology (MEST) and the Korea Research Foundation Grant funded by the Korean Government (MOEHRD) (KRF-2006-331-C00202 and KRF-2008-314-C00234).

6. References

- [1] R. E. Ionescu, C. Gondran, L. A. Gheber, S. Cosnier, R. S. Marks, *Anal. Chem.* **2004**, *76*, 6808.
- [2] R. E. Ionescu, C. Gondran, S. Cosnier, L. A. Gheber, R. S. Marks, *Talanta* **2005**, *66*, 15.
- [3] P. Fanjul-Bolado, M. B. González-García, A. Costa-García, *Anal. Bioanal. Chem.* **2005**, *382*, 297.
- [4] G. Volpe, D. Compagnone, R. Draisci, G. Palleschi, *Analyst* **1998**, *123*, 1303.
- [5] A. Crew, C. Alford, D. C. C. Cowell, J. P. Hart, *Electrochim. Acta* **2007**, *52*, 5232.
- [6] W. Sun, K. Jiao, S. Zhang, C. Zhang, Z. Zhang, *Anal. Chim. Acta* **2001**, *434*, 43.
- [7] A. Preechaworapun, Z. Dai, Y. Xiang, O. Chailapakul, J. Wang, *Talanta* **2008**, *76*, 424.
- [8] M. S. Wilson, R. D. Rauh, *Biosens. Bioelectron.* **2004**, *20*, 276.
- [9] P. Fanjul-Bolado, D. Hernández-Santos, M. B. González-García, A. Costa-García, *Anal. Chem.* **2007**, *79*, 5272.
- [10] S. Hwang, E. Kim, J. Kwak, *Anal. Chem.* **2005**, *77*, 579.
- [11] J. Das, K. Jo, J. W. Lee, H. Yang, *Anal. Chem.* **2007**, *79*, 2790.
- [12] M. A. Aziz, S. Park, S. Jon, H. Yang, *Chem. Commun.* **2007**, 2610.
- [13] M. A. Aziz, S. Patra, H. Yang, *Chem. Commun.* **2008**, 4607.
- [14] S. J. Kwon, H. Yang, E. Kim, J. Kwak, *Analyst* **2008**, *133*, 1599.
- [15] R. E. Gyurcsányi, A. Bereczki, G. Nagy, M. R. Neuman, E. Lindner, *Analyst* **2002**, *127*, 235.
- [16] L. D. Mello, M. D. P. T. Sotomayor, L. T. Kubota, *Sens. Actuators B* **2003**, *96*, 636.
- [17] L. Dill, D. D. Montgomery, A. L. Ghindilis, K. R. Schwarzkopf, S. R. Ragsdale, A. V. Oleinikov, *Biosens. Bioelectron.* **2004**, *20*, 736.
- [18] D. Du, F. Yan, S. Liu, H. Ju, *J. Immunol. Meth.* **2003**, *283*, 67.
- [19] M. A. Aziz, T. Selvaraju, H. Yang, *Electroanalysis* **2007**, *19*, 1543.
- [20] J. Stotter, Y. Show, S. Wang, G. Swain, *Chem. Mater.* **2005**, *17*, 4880.
- [21] A. N. Asanov, W. W. Wilson, P. B. Oldham, *Anal. Chem.* **1998**, *70*, 1156.
- [22] I. Zudans, J. R. Paddock, H. Kuramitz, A. T. Maghasi, C. M. Wansapura, S. D. Conklin, N. Kaval, T. Shtoyko, D. J. Monk, S. A. Bryan, T. L. Hubler, J. N. Richardson, C. J. Seliskar, W. R. Heineman, *J. Electroanal. Chem.* **2004**, *565*, 311.
- [23] J. Peng, Z.-N. Gao, *Anal. Bioanal. Chem.* **2006**, *384*, 1525.
- [24] H. Qi, C. Zhang, *Electroanalysis* **2005**, *17*, 832.

Wiley-VCH BOOK SHOP



M. Reiher / A. Wolf
Relativistic Quantum Chemistry
 The Fundamental Theory of Molecular Science

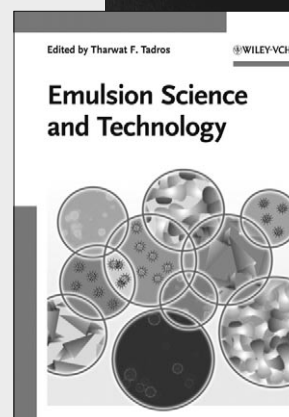
Written by two researchers, this book presents the fascinating field of relativistic quantum chemistry in a unique, self-contained way. For the first time this new topic is combined in one book, essential for theoretical chemists and physicists.

690 pp, cl, € 159.00
 ISBN: 978-3-527-31292-4

T. F. Tadros (ed.)
Emulsion Science and Technology

Highlighting recent developments as well as future challenges, this book covers a wealth of topics from Nanoparticles Synthesis to Nanocomposites to Cosmetic Emulsions. Essential guide for those involved in Formulations Technology.

344 pp, cl, € 119.00
 ISBN: 978-3-527-32525-2



Prices are subject to change without notice.

You can order online via <http://www.wiley-vch.de>
 Wiley-VCH Verlag GmbH & Co. KGaA · POB 10 11 61 · D-69451 Weinheim, Germany
 Phone: 49 (0) 6201/606-400 · Fax: 49 (0) 6201/606-184 · E-Mail: service@wiley-vch.de

 WILEY-VCH